Available online at www.sciencedirect.com
SCIENCE DIRECT®
Journal of Power Sources 119–121 (2003) 701–705
JOURNAL OF POWER SOURCES
www.elsevier.com/locate/jpowsour

Structure stabilization of $LiMn_2O_4$ cathode material by bimetal dopants

Y.W. Tsai[a], R. Santhanam[a], B.J. Hwang[a,*], S.K. Hu[b], H.S. Sheu[c]

[a]*Microelectrochemistry Laboratory, Department of Chemical Engineering, National Taiwan University of Science and Technology, Keelung Road, Section 4, Taipei 106, Taiwan, ROC*
[b]*Department of Chemical Engineering, National Cheng Kung University, Tainan 701, Taiwan, ROC*
[c]*National Synchrotron Radiation Research Center, Hsinchu 300, Taiwan, ROC*

Abstract

The structural changes of spinel $Li_{1.02}Mn_2O_4$ and $Li_{1.02}Co_{0.11}Ni_{0.04}Mn_{1.85}O_4$ cathode materials have been studied by synchrotron powder X-ray diffraction and differential scanning calorimetry (DSC) measurements. The results show that spinel $Li_{1.02}Mn_2O_4$ undergoes a phase transition from cubic (*Fd3m*) to orthorhombic symmetry (*Fddd*) at $T = 285$ K. However, substitution of a small amount of Co^{3+} and Ni^{3+} ions suppresses phase transition and the cubic phase is maintained at low temperature due to a decrease in the concentration of Jahn–Teller active Mn^{3+} ions.

Keywords: $LiMn_2O_4$; Bimetal substitution; X-ray diffraction; Differential scanning calorimetry

1. Introduction

Transition metal oxides, especially $LiMn_2O_4$, $LiCoO_2$ and $LiNiO_2$ have been studied extensively as cathode materials for rechargeable lithium batteries [1–5]. Among these three oxides, $LiMn_2O_4$ and its derivatives are considered as promising cathode materials because of advantages such as low cost, abundance, high specific energy and environmental friendly nature [6–8]. Spinel $Li_xMn_2O_4$ mainly exhibits two voltage plateaus, 4 V for $0 < x \leq 1$ and 3 V for $1 < x \leq 2$. The cubic structure of the spinel $LiMn_2O_4$ is maintained when it is cycled in the 4 V range. On the other hand, severe capacity fading is observed in the 3 V range due to a structural phase transformation from cubic to tetragonal, resulting from a Jahn–Teller distortion of the Mn^{3+} ions. Even though the cycling performance of spinel $LiMn_2O_4$ electrode is far better in the 4 V range than 3 V range, it shows considerable capacity fading in the 4 V range also, on long-term cycling. The capacity fading of the material has been attributed to several factors, such as (1) dissolution of manganese into the electrolyte and decomposition of the electrolyte [9–11], (2) cation mixing between Li and Mn ion in the spinel lattice [12], (3) oxygen loss from the spinel lattice [13]and (4) break down of the spinel lattice [14]. Among various approaches to overcome these problems, one effective approach is to substitute a small amount of dopant ions instead of Mn ions [15–18]. It is believed that the dopant ions occupy 16*d* sites of Mn-ions in the spinel lattice and stabilize the spinel structure.

Since Mn contains Mn^{4+} ($t_{2g}^3 e_g^0$) and Jahn–Teller active Mn^{3+} ($t_{2g}^3 e_g^1$) ions, decreasing the temperature results in structural phase transitions of $LiMn_2O_4$ due to the Jahn–Teller distortion on the Mn^{3+} sites with the appearance of mixture of cubic and tetragonal phases [19–21]. The original studies were unclear about whether the low temperature form was tetragonal or orthorhombic, but later studies unequivocally showed that in fact the orthorhombic structure was formed [22,23]. As far as battery applications are concerned, unwanted phase transitions close to room temperature should be avoided to get excellent cycling capacity. More recently, we reported a better cycling performance for the bimetal doped (Co, Ni) spinel $LiMn_2O_4$ compared to that of undoped one [24]. In this paper, the phase transitions are investigated in $Li_{1.02}Mn_2O_4$ and $Li_{1.02}Co_{0.11}Ni_{0.04}Mn_{1.85}O_4$ at low temperatures.

2. Experimental

$Li_{1.02}Mn_2O_4$, and $LiCo_{0.11}Ni_{0.04}Mn_{0.85}O_4$ were synthesized by a sol–gel method using citric acid as a chelating agent [25,26]. The molar ratio of total metal ions:citric

* Corresponding author. Tel.: +886-2-27376624; fax: +886-2-27376644.
E-mail address: bjh@ch.ntust.edu.tw (B.J. Hwang).

0378-7753/03/$ – see front matter
doi:10.1016/S0378-7753(03)00226-X

acid = 1:1. Stoichiometric amounts of $Li(CH_3COO)\cdot 4H_2O$, and $Mn(CH_3COO)_2\cdot 4H_2O$, and $Li(CH_3COO)\cdot 4H_2O$, $Mn(CH_3COO)_2\cdot 4H_2O$, $Ni(CH_3COO)_2\cdot 4H_2O$, and $Co(NO_3)_2\cdot 4H_2O$, respectively, were dissolved in distilled water. The temperature was maintained at 35 °C. The solution pH was adjusted to 6.0 with ammonium hydroxide. The entire process was carried out under continuous stirring. The prepared solution was heated in a beaker on a hot plate in the temperature range of 80–90 °C for 4 h until a transparent sol was obtained. The resulting gel precursor was decomposed at 400 °C for 4 h in oxygen to remove the organic contents. The decomposed powders were ground, pressed as pellets and calcined at 800 °C in oxygen for 10 h. The heating rate of the powder was 2 °C/min and furnace cooled.

Li, Co, Ni, and Mn contents in the resulting materials were analyzed using an inductively coupled plasma/atomic emission spectrometer (ICP/AES, Kontron S-35). Differential scanning calorimetry (DSC) was performed under a constant heat flow. Data were collected between 373 and 263 K with heating and cooling rates of 20 K/min.

XRD studies were performed on the beam line 17A at the National Synchrotron Radiation Research Center (NSRRC) in Taiwan operated at an energy of 9 keV ($\lambda = 1.32633$ Å). All of the XRD diffraction patterns were recorded in a limited angular region at various temperatures. The optical design follows a first mirror focusing the beam vertically and an asymmetrically cut and horizontally bendable perfect single crystal as the diffraction object monochromatizing and focusing the beam horizontally. A single crystal of Si(1 1 1) with about 10% asymmetric cutting was used to deliver the monochromatic beam. The optics are designed to focus the beam into a 0.1 mm × 3 mm spot size at the sample position, which is about 24 m away from the source or 6 m from the monochromator. The wavelength of the beam is 1.32633 Å. A flat imaging plane (Fuji, 20 cm × 40 cm) was used as a 2-D area detector, which can collect diffraction data up to 80° in 2θ. The diffraction pattern was read out by using a MAC IPR420 off line imaging plate scanner. The dynamic range is as high as 10^6. In this study, the sample was cooled by an APD cryostat; the temperature varied from 300 to 25 K.

3. Results and discussion

The synchrotron powder X-ray diffraction patterns of $Li_{1.02}Mn_2O_4$ during cooling process in the 30–46° (2θ) range at different temperatures from 300 to 25 K are shown in Fig. 1. As can be seen in this figure, the (4 0 0) reflection around 2θ value 37.48° of the *Fd*3*m* cubic spinel splits into (4 0 0), (0 4 0) and (0 0 4) reflections of the orthorhombic *Fddd* phase below 285 K. The (3 1 1) reflection at 2θ splits into (3 1 1), (1 3 1) and (1 1 3) reflections. The broadening of the (3 3 1) peak at 2θ value 30.91° below 285 K is due to its splitting of closely spaced reflections (3 3 1), (3 1 3) and (1 3 3). It is clear that the cubic to orthorhombic phase transition begins at 285 K and continues until 25 K during cooling process. Fig. 2 shows the synchrotron XRD pattern of a $Li_{1.02}Co_{0.11}Ni_{0.04}Mn_{1.85}O_4$ sample. This figure shows the cubic spinel peaks (3 1 1), (2 2 2), (4 0 0) and (3 3 1) in the 2θ range 30–44° from 300 to 40 K during the cooling process. It is clearly seen that there is no peak splitting from room temperature, 300 K to a low temperature, 40 K. This means that the reduction of the concentration of Mn^{3+} ions by small amount of bimetal dopants substitution results in the suppression of the Jahn–Teller distortion in $Li_{1.02}Co_{0.11}Ni_{0.04}Mn_{1.85}O_4$ and the cubic phase is retained at low temperature. Fig. 3 shows the temperature dependence of relative area of the (0 4 0) peak indexed by the space group

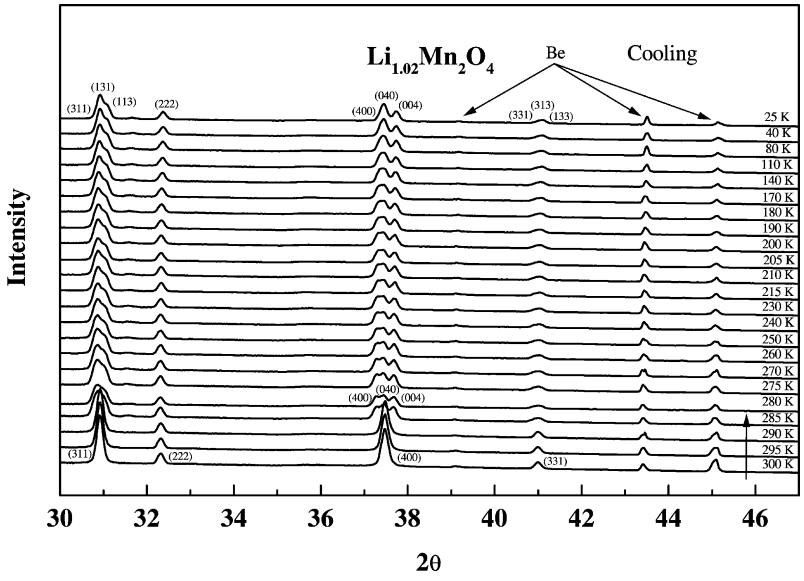

Fig. 1. Powder X-ray diffraction pattern of $Li_{1.02}Mn_2O_4$ at 2θ in the 30–46° region, recorded between 300 and 25 K; synchrotron wavelength 1.32633 Å.

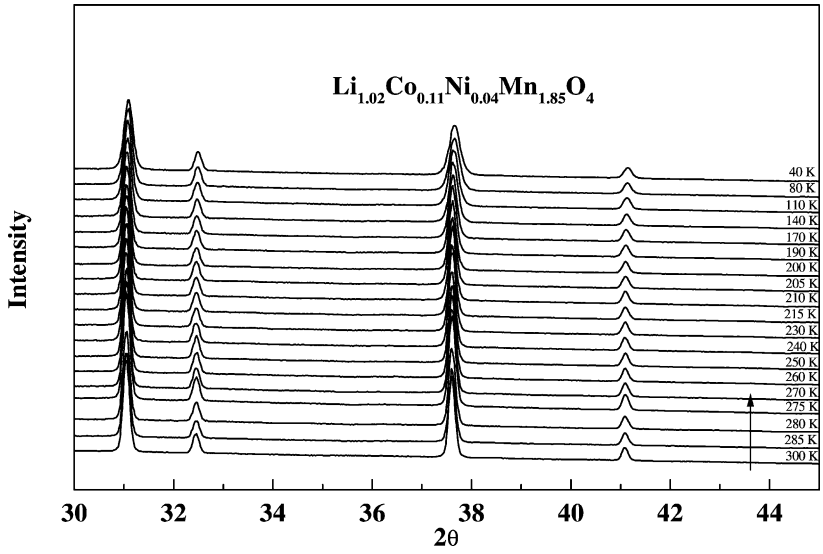

Fig. 2. Powder X-ray diffraction pattern of $Li_{1.02}Co_{0.11}Ni_{0.04}Mn_{1.85}O_4$ at 2θ in the 30–46° region, recorded between 300 and 40 K; synchrotron wavelength 1.32633 Å.

Fddd and the (1 1 1) peak indexed by *Fd*3*m*, and also the relative area of the (4 0 0) peak indexed by *Fd*3*m* and (1 1 1) indexed by *Fd*3*m* for the $Li_{1.02}Mn_2O_4$ material. On cooling, the transformation to orthorhombic $Li_{1.02}Mn_2O_4$ can be seen around 280 K (Fig. 3). This type of cubic to orthorhombic transition was not observed, from the temperature dependence of relative area measurements, in the case of $Li_{1.02}Co_{0.11}Ni_{0.04}Mn_{1.85}O_4$ material.

In order to further analyze the phase transition in $Li_{1.02}Mn_2O_4$ and suppression of the phase transition in the case of $Li_{1.02}Co_{0.11}Ni_{0.04}Mn_{1.85}O_4$, DSC experiments were carried out in the temperature range between 373 and 263 K and are shown in Fig. 4a and b, respectively, during the cooling process. The materials used for DSC measurements were synthesized at 800 °C in oxygen for 10 h. The exothermic peak observed for $Li_{1.02}Mn_2O_4$ about 281 K corresponds to the structural phase transition from cubic (*Fd*3*m*) to orthorhombic (*Fddd*) caused by the Jahn–Teller effect of Mn^{3+} ions. However, the phase transition is suppressed when some manganese is replaced by cobalt and nickel ions as shown in Fig. 4b.

Note that only a small amount of Co, Ni substitution for Mn has a significant effect on the phase transition behavior. The Mn^{3+} content decreases due to the substitution of Co^{3+} and Ni^{3+} on the 16*d* site of $LiMn_2O_4$ framework and thus brings about changes in the local ordering. It is clear from these results that the Jahn–Teller distortion is smaller in $Li_{1.02}Co_{0.11}Ni_{0.04}Mn_{1.85}O_4$ than in $Li_{1.02}Mn_2O_4$,

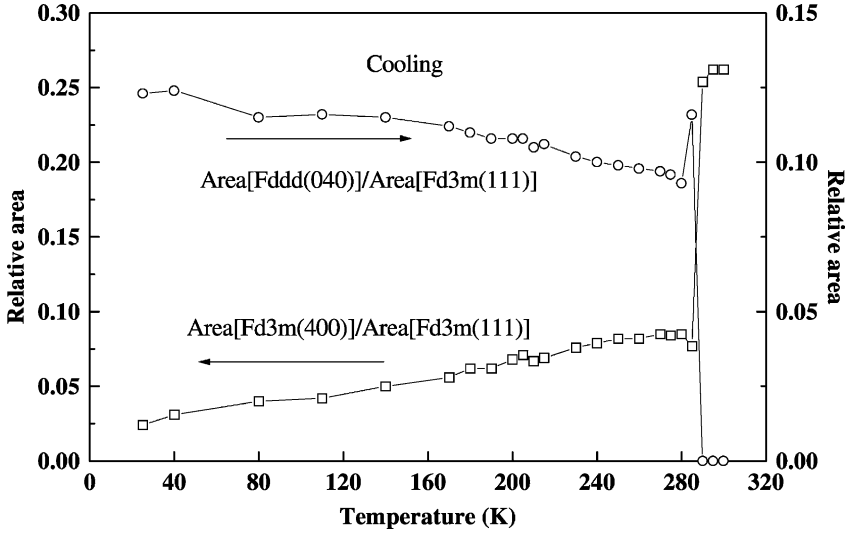

Fig. 3. Relative area of *Fddd*(0 4 0)/*Fd*3*m*(1 1 1) and *Fd*3*m*(4 0 0)/*Fd*3*m*(1 1 1) as a function of temperature in $Li_{1.02}Mn_2O_4$.

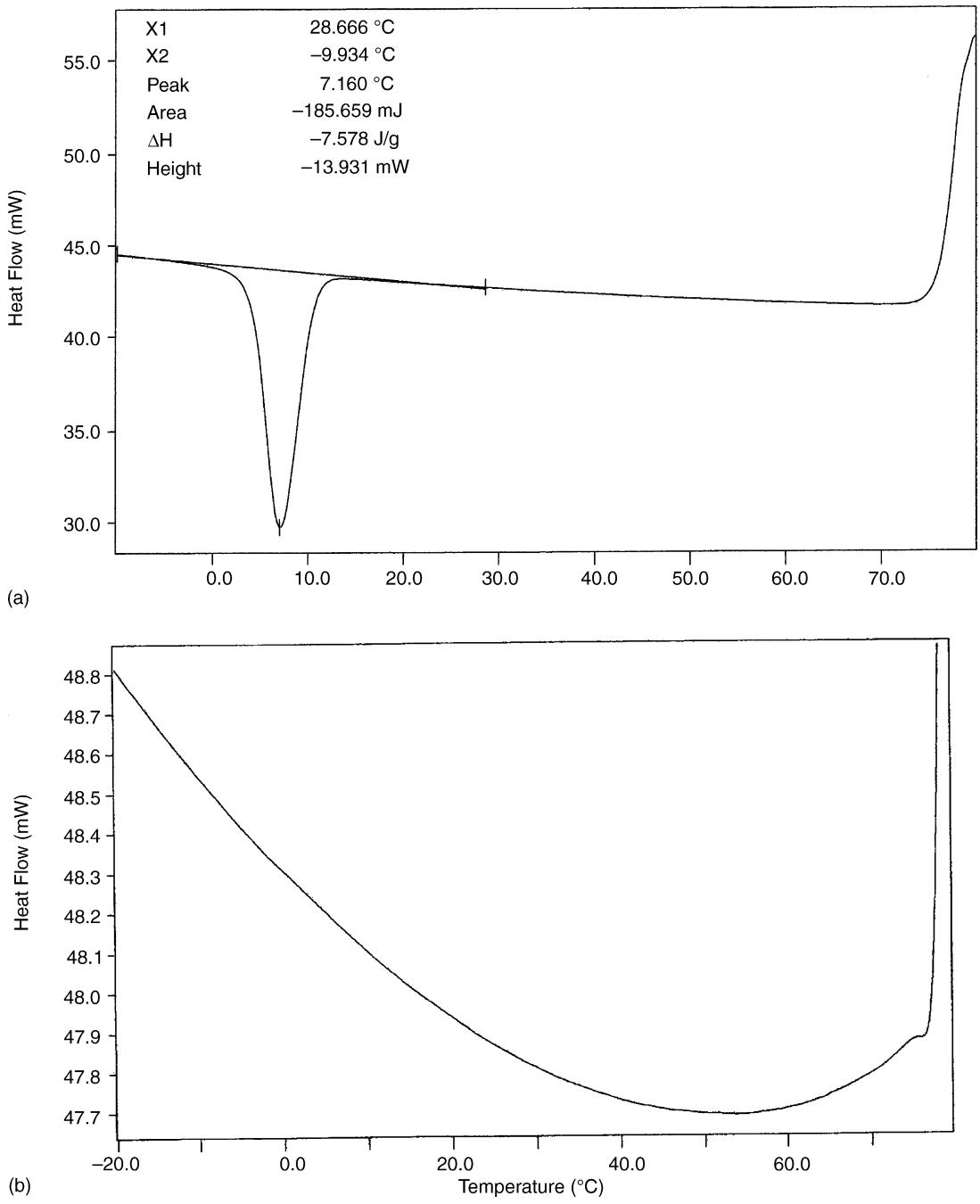

Fig. 4. DSC curves measured in the temperature range 280 K during cooling process for (a) $Li_{1.02}Mn_2O_4$ and (b) $LiCo_{0.11}Ni_{o.04}$ $Mn_{1.85}O_4$ cathode materials.

leading to a less ordered local structure in the former. From the results obtained in this work, it seems that the disordering of the [MnO_6] octahedra is much smaller in $Li_{1.02}Co_{0.11}Ni_{0.04}Mn_{1.85}O_4$ than that of $Li_{1.02}Mn_2O_4$.

4. Conclusions

The phase transitions of two cathode materials, $Li_{1.02}$-Mn_2O_4 and $Li_{1.02}Co_{0.11}Ni_{0.04}$ $Mn_{1.85}O_4$ materials were investigated at different temperatures from room temperature to a low temperature during cooling process. Synchrotron X-ray diffraction and differential scanning calorimetry studies indicated that $Li_{1.02}Mn_2O_4$ shows a phase transition at 285 K that is related to the cubic to orthorhombic transition. However, substitution of small amount of Co^{3+} and Ni^{3+} ions reduces the concentration of Jahn–Teller active Mn^{3+} ions and hence suppresses the phase transition and the cubic phase is maintained at low temperatures.

Acknowledgements

The financial support from National Science Council (NSC 89-2214-E-011-044 and NSC 90-2811-E-011-005) and Education Ministry (EX-91-E-FA09-5-4), National Synchrotron Radiation Research Center (NSRRC), Hsinchu and National Taiwan University of Science and Technology, Taiwan, Republic of China is gratefully acknowledged.

References

[1] M.M. Thackeray, P.J. Johnson, L.A. de Picciotto, P.G. Bruce, J.B. Goodenough, Mat. Res. Bull. 19 (1984) 179.
[2] W. Li, J.C. Curie, J. Electrochem. Soc. 144 (1997) 2773.
[3] R.J. Gummow, A. de Kock, M.M. Thackeray, Solid State Ionics 69 (1994) 59.
[4] E. Plichita, M. Salomon, S. Slane, M. Uchiyama, J. Power Sources 21 (1987) 25.
[5] J. Cho, J. Guan, M. Liu, Solid State Ionics 95 (1997) 289.
[6] M.M. Thackeray, Prog. Solid State Chem. 25 (1997) 1.
[7] S. Megahed, B. Scrosati, J. Power Sources 51 (1994) 79.
[8] T. Ohzuku, M. Kitagawa, T. Hirai, J. Electrochem. Soc. 137 (1990) 769.
[9] Y. Xia, Y. Zhou, M. Yoshio, J. Electrochem. Soc. 144 (1997) 2593.
[10] D.H. Jang, Y.J. Shin, S.M. Oh, J. Electrochem. Soc. 143 (1996) 2204.
[11] D.H. Jang, S.M. Oh, J. Electrochem. Soc. 144 (1997) 3342.
[12] Y. Xia, M. Yoshio, J. Electrochem. Soc. 143 (1996) 825.
[13] Y. Xia, T. Sakai, T. Fujieda, X.Q. Yang, X. Sun, Z.F. Ma, J. McBreen, M. Yoshio, J. Electrochem. Soc. 148 (2001) A723.
[14] Y. Xia, M. Yoshio, J. Electrochem. Soc. 143 (1996) 825.
[15] Y. Ein-Eli, J.T. Vaughty, M.M. Thackeray, S. Mukerjee, X.Q. Yang, J. McBreen, J. Electrochem. Soc. 146 (1999) 908.
[16] J.H. Lee, J.K. Hong, D.H. Jang, Y.K. Sun, S.M. Oh, J. Power Sources 89 (2000) 7.
[17] N. Hayashi, H. Ikuda, M. Wakihara, J. Electrochem. Soc. 146 (1999) 1351.
[18] Y. Ein-Eli, W.F. Howard, J. Electrochem. Soc. 144 (1997) L205.
[19] A. Yamada, M. Tanaka, Mat. Res. Bull. 30 (1995) 715.
[20] H. Yamaguchi, A. Yamada, H. Uwe, Phys. Rev. B 58 (1998) 8.
[21] A. Yamada, J. Solid State Chem. 122 (1996) 160.
[22] H. Hayakawa, T. Takada, H. Enoki, E. Akiba, J. Mat. Sci. Lett. 17 (1998) 811.
[23] G. Rousse, C. Masquelier, J. Rodriguez-Carvajal, M. Hervien, Electrochem. Solid State Lett. 2 (1999) 6.
[24] B.J. Hwang, R. Santhanam, S.G. Hu, J. Power Sources 108 (2002) 250.
[25] J.H. Choy, D.H. Kim, C.W. Kwon, S.J. Hwang, Y.I. Kim, J. Power Sources 77 (1999) 1.
[26] B.J. Hwang, R. Santhanam, D.G. Liu, J. Power Sources 97–98 (2001) 443.